Computer Speech and Language (1989) **3**, 105–118

Digital filter simulation of the basilar membrane

Eliathamby Ambikairajah

Department of Electronic Engineering, Regional Technical College, Athlone, Eire

Norman D. Black

Department of Electrical & Electronic Engineering, Biomedical Research Centre, University of Ulster at Jordanstown, Shore Road, Newtownabbey, Co. Antrim BT37 0QB, N. Ireland

and

Robert Linggard

Continuous Speech Recognition Group, British Telecom Research Labs., Martlesham Heath, Ipswich, U.K.

Abstract

This paper describes a digital filter simulation of basilar membrane vibration, in which the cochlea is represented as a cascade of 128 filters. The parameters of each filter are determined from the mechanical characteristics of the basilar membrane at corresponding points. Using this model, it is possible to simulate, at each point, the waveform of the sound pressure in the cochlear fluid, as well as the deflection of the membrane itself. A significant advantage of this practical model is that the computation time is considerably shortened in comparison with other similar models and it thus has application as a front-end processor in speech recognition systems.

This work can be used as a basis for developing a cochlear model which includes active elements in the cochlea in line with the most recent findings in this field.

1. Introduction

The cochlea of the human ear is amongst the most integrated and sophisticated organs of the body. Buried deep in the temporal bone of the skull, it performs spectral analysis and neural encoding of the acoustic waveform. However, its inaccessibility makes it one of the least understood organs. Researchers, in attempting to improve the understanding of cochlear function, have employed cochlear modelling techniques. Cochlear models described in the literature can generally be classified into one of two broad categories:

(i) analytical;
(ii) computational.

0885-2308/89/020105+14 $03.00/0

Analytical models succinctly capture the behaviour of the cochlea by faithfully reproducing its response to any given stimulus, and may be used to give valuable insight into the mysterious operation of the cochlea itself. Analytical models can be classified as either single (1-D) or multi-dimensional (2-D, 3-D) types.

Computational models differ from analytical models in that they mimic relevant behaviour of the auditory system, but not necessarily in a strict physiological way. Their area of application is quite different from the analytical models, being useful in engineering systems, such as acoustic analysers in automatic speech recognizers. Unlike the analytical models, computational models must necessarily be computationally efficient.

Two computational models based on the mathematical model of Zweig, Lipes & Pierce (1976) are of merit because of their roughly physiological basis. These models, described by Lyon (1982) and Dolmazon, Bastet & Shuplakov (1977), use the same filter structure consisting of a cascade of second-order filters to represent the travelling pressure waves in the cochlea, and a parallel collection of second-order resonators which convert the pressure waves into basilar membrane (BM) motion. The two models differ in that Dolmazon *et al.* use second-order low-pass filters as the series element, whereas Lyon uses second-order notch filters. The main physiological feature of these models is that both are able to match the amplitude characteristics which Rhode (1971) observed, simply by adjusting the circuit elements of the filters.

Lyon, in particular, has extensively exploited his model using additional physiologically plausible post-processing to investigate several psychoacoustic phenomena with good success. One disadvantage of these models, however, is the difficulty in using them to obtain the equivalent circuit for one section of the BM in terms of fluid mass, fluid volume velocity, etc. A preliminary study by Black (1983), and Ambikairajah & Linggard (1984), has shown that it is possible to design a model which does have a physiological basis and yet is computationally efficient.

In this paper, a practical model of the cochlea, consisting of 128 sections, is now proposed. It will be demonstrated that this model exhibits classical observations such as travelling waves etc., and is capable of producing amplitude responses which are in good agreement with those obtained empirically by Rhode (1971). It will be shown further that either the Lyon or Dolmazon *et al.* models can be derived from the proposed cochlear model.

The purpose of this work is to arrive at a practical model of the cochlea, using modifications of the linear 1-D transmission line proposed by Schroeder (1973). The model is designed with the following goals in mind:

(i) from the model, it should be possible to obtain an equivalent circuit of a section of the BM in terms of fluid mass, fluid volume velocity, etc.;
(ii) the results of the model should be in good agreement with the experimental data of the BM vibration;
(iii) the model should be as simple as possible so that it is computationally attractive.

2. A one-dimensional model of the cochlea

2.1. Development of the model

In accordance with previous work in this field (Schroeder, 1973), the motion of the BM is described as a transmission line with distributed parallel and series impedances that vary

continuously with distance, x, along the membrane. The voltage at any point on this transmission line is analogous to the pressure in the cochlear fluid and the current is analogous to the volume velocity of the fluid.

A simplified electrical model of a section of the BM is shown in Fig. 1. The model parameters are described as follows:

series inductance	$M = m(x)\Delta x$
shunt inductance	$L = l(x)/\Delta x$
shunt capacitance	$C = c(x)\Delta x$
shunt resistance	$R = r(x)/\Delta x$

Δx length of the BM section

$m(x)$ inductance which represents the mass of fluid which moves in a horizontal (longitudinal) direction, parallel to the BM

$l(x)$ inductance which represents the mass of the BM, associated structures and vertically (laterally) moving fluid

$r(x)$ resistance which represents losses associated with motion of the membrane

$c(x)$ capacitance which represents the compliance of the membrane

The charge, $Q(x)$, on the capacitor represents the displacement of the membrane.

The dynamic behaviour of the BM may be calculated by approximating the distributed transmission line by a cascade connection of N short sections, with the parameters M, L, C, and R dependent on the position, x, along the membrane. The behaviour of this cascade connection will approach that of the true distributed system as $\Delta x \to 0$, that is, as N (number of sections) is made very large.

The complete model for the motion of the BM would be as shown in Fig. 2. For large N, the analysis of this electrical model is a tedious procedure. In order to make the computational task more tractable, it would be convenient if each section was to be isolated from its neighbours. This isolation can be achieved if the interaction between sections is taken into account by considering each section to be loaded by a shunt impedance (Z_T) which represents the input impedance of the remainder of the membrane.

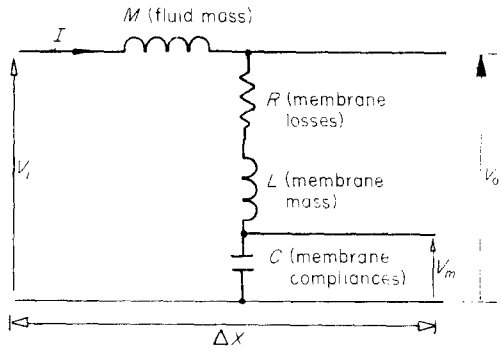

Figure 1. An electrical model of one section of the basilar membrane. v_i and v_o represent the input and output pressure differences between the scalae, respectively, and v_m is the voltage which is proportional to the membrane displacement. Δx is the length of the basilar membrane section.

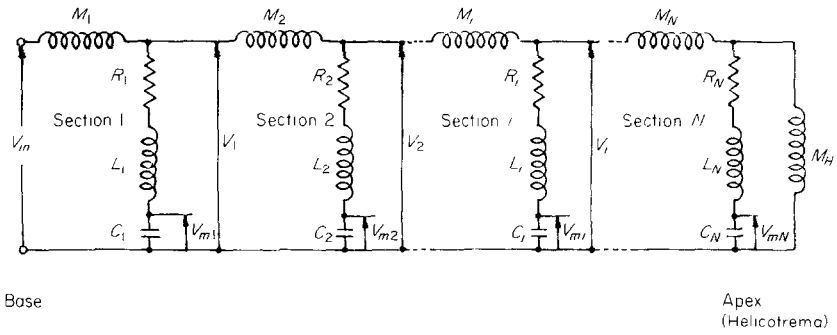

Figure 2. The cascade model for the motion of the basilar membrane represented by N sections.

According to Dallos (1973), Z_T has a significant reactive component at low frequencies which is due to the acoustic behaviour of the helicotrema. If the acoustic impedance of the helicotrema is represented by $Z_h = R_h + j\omega M_h$, then Z_h shunts some acoustic resistance R_c which represents the input impedance of the cochlea without the contribution of the helicotrema. Therefore the total impedance Z_T is given by:

$$Z_T = \frac{R_c(R_h + j\omega M_h)}{R_c + R_h + j\omega M_h}. \tag{1}$$

From (1) it is clear that at high frequencies the impedance tends towards R_c. Thus the high-frequency input impedance is independent of the helicotrema, while the low-frequency value is strongly dependent on it.

A considerable simplification occurs if the shunt impedance Z_T is approximated by a simple parallel connection of an inductance M_T and a resistance R_T. This approximation has such a small effect on the overall characteristics of the model that it may be ignored. This simplification leads to the isolated section shown in Fig. 3(a), where the isolation is achieved by inclusion of an isolation amplifier. The voltage transfer function of the whole line would then be simply the product of the transfer functions for each section. The pressure transfer function, $v_o(s)/v_i(s)$, can be obtained by analysing the network shown in Fig. 3(a).

Applying Thevenin's theorem across points A and B, the network shown in Fig. 3(b) is obtained, where v_{The} and z_{The} are the Thevenin voltage and impedance given by:

$$v_{\text{The}} = v_i * \frac{R_T/M}{j\omega + R_T/L_T},$$

$$z_{\text{The}} = j\omega M // j\omega M_T // R_T \tag{2}$$

$$= \frac{j\omega R_T}{j\omega + R_T/L_T},$$

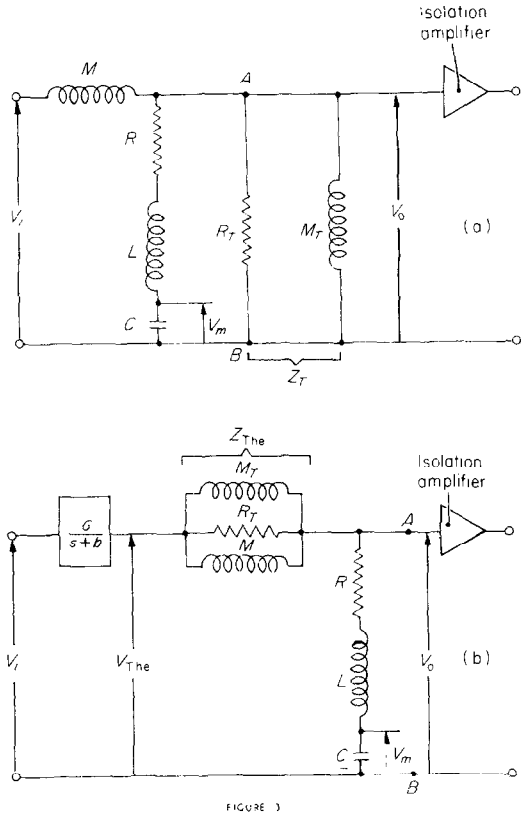

Figure 3. Simplified electrical models of one section of the basilar membrane. (a) How the loading effects of succeeding sections can be modelled. (b) Resulting model for one section in which the pressure transfer function is v_o/v_i and the displacement transfer function is v_m/v_i.

where

$$L_T = \frac{MM_T}{M+M_T}.$$

The transfer function $v_{\text{The}}(s)/v_i(s)$ obtained from (2) is seen to be a low-pass function of the form $G/(s+b)$. The voltage transfer function $v_o(s)/v_{\text{The}}(s)$ can be obtained from Fig. 3(b) and is given by:

$$\frac{v_o(s)}{v_{\text{The}}(s)} = \frac{\left(s+\frac{R_T}{L_T}\right)\left(s^2+\frac{R}{L}s+\frac{1}{LC}\right)}{s^3+\left(\frac{R_T}{L}+\frac{R_T}{L_T}+\frac{R}{L}\right)s^2+\left(\frac{1}{LC}+\frac{RR_T}{LL_T}\right)s+\frac{R_T}{LL_TC}}. \tag{3}$$

In order to have a resonant pole frequency, the denominator in (3) should have a pair of

complex poles. As a result it can be written as the product of first- and second-order poles.

The voltage, or pressure transfer function of the isolated section can be obtained by combining (2) and (3) to give:

$$\frac{v_o(s)}{v_i(s)} = K * \frac{a}{s+a} * \frac{\omega_p^2}{s^2 + B_p s + \omega_p^2} * \frac{s^2 + B_z s + \omega_z^2}{\omega_z^2}. \tag{4}$$

s complex frequency variable
K attenuation factor
a low-pass pole frequency
ω_p resonant pole frequency
B_p pole bandwidth
ω_z resonant zero frequency with $\omega_z > \omega_p$
B_z zero bandwidth

Equation (4) highlights the fact that the pressure transfer function of one section of the membrane consists of a low-pass function, a resonant pole, and a resonant zero. The filtering action of a particular section will thus have three consequences:

(1) frequencies below the pole frequency ω_p will pass attenuated by the factor K;
(2) frequencies close to the pole frequency will be enhanced;
(3) frequencies at or above the zero frequency ω_z will be attenuated quite severely.

Although $\omega_z > \omega_p$, in reality the values are quite close.

The actual displacement of the BM is analogous to the charge on the capacitor C and it is proportional to the voltage v_m shown in Fig. 1. The displacement transfer function is given by:

$$\frac{v_m(s)}{v_i(s)} = K * \frac{a}{s+a} * \frac{\omega_p^2}{s^2 + B_p s + \omega_p^2}. \tag{5}$$

It can be seen that the low-pass filter function given in (5) is exactly like the pressure transfer function of (4), but without the resonant zero. The displacement at any point x on the basilar membrane can thus be calculated by taking the product of the pressure transfer functions up to that point, and then multiplying by the displacement transfer function at that particular point x.

2.2. Filter parameters

If appropriate values of the filter parameters K, a, ω_p, ω_z, and B_z are used in each filter section, the response of the whole BM can be quite realistic. Unfortunately, the filter parameters cannot be obtained explicitly in terms of the network element values M, R, L, C, M_T, and R_T. In addition, the element values themselves are not all known accurately, since they are electrical analogues of the mechanical properties of the cochlea. One way of obtaining filter parameters is discussed below.

The electrical model of the isolated section, as shown in Fig. 4, results if the reactive component M_T in Fig. 3(a) is Thevenized across A and B. The transfer function of Fig. 4 is given by:

$$\frac{v_o(s)}{v_i(s)} = \frac{R_T *}{L_T} \frac{s^2 + \left(\frac{R}{L}\right) s + \left(\frac{1}{LC}\right)}{s^3 + \left(\frac{R_T}{L} + \frac{R_T}{L_T} + \frac{R}{L}\right) s^2 + \left(\frac{1}{LC} + \frac{RR_T}{LL_T}\right) s + \frac{R_T}{LL_T C}}. \tag{6}$$

The transfer function of the original section is given by (4) and can be rewritten as:

$$\frac{v_o(s)}{v_i(s)} = \frac{\omega_p^2 *}{\omega_z^2} \frac{a(s^2 + B_z s + \omega_z^2)}{s^3 + (B_p + a)s^2 + (\omega_p^2 + B_p a)s + a\omega_p^2}. \tag{7}$$

The transfer functions given in (6) and (7) are equivalent. For convenience we define two ratios,

$$r = \frac{\omega_z}{\omega_p} \quad \text{and} \quad p = \frac{a}{\omega_z}. \tag{8}$$

It is also known that

$$Q_p = \frac{\omega_p}{B_p} \quad \text{and} \quad Q_z = \frac{\omega_z}{B_z}, \tag{9}$$

where Q_p and Q_z are Q-factors associated with the poles and zeros of the functions.

By equating (6) and (7) and using (8) and (9), we obtain the following relationships in terms of r, p, and network elements:

$$\frac{r^2 - 1}{p^2} * \left(p^2 - \frac{pr}{Q_p} + r^2\right) = \frac{L_T}{L}, \tag{10}$$

$$\frac{r^2 - 1}{p^2} * \left(p^2 - \frac{p}{Q_z} + 1\right) = \frac{L_T}{L}, \tag{11}$$

$$\frac{r}{Q_p} - \frac{1}{Q_z} = \frac{r^2 - 1}{p}. \tag{12}$$

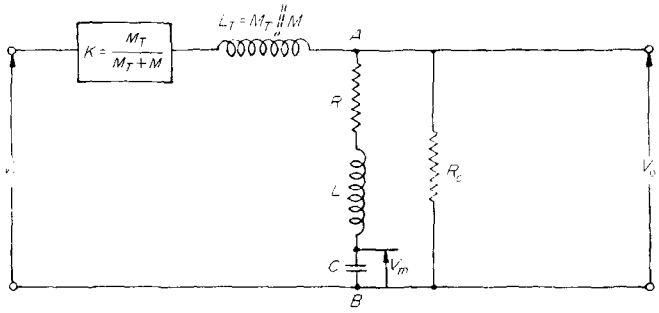

Figure 4. The electrical model of the isolated section which results if the reactive component M_T is Thevenized across A and B in Fig. 3(a).

Equations (10), (11), and (12) are non-linear. These equations can be solved by putting constraints on the values of a, ω_p, and B_p and hence on the values of Q_p and p.

This model assumes that the ratio L_T/L given in (10) and (11) is small. It is difficult to estimate the ratio of L_T/L accurately, since there are variations in the reported compliance measurements of the BM. A useful procedure for determining appropriate values for r and p (and hence ω_p and a) is as follows:

(i) Choose values for Q_p and Q_z which reflect accurately the losses of each section, based on reported experimental results. The values in the range of

$$10 < Q_z < \infty \quad \text{and} \quad 1 < Q_p < 20$$

are found to be appropriate.

(ii) Use (12) to select compatible values for r and p. The following ranges of values for r and p satisfy (10), (11), and (12):

$$1{\cdot}01 < r < 1{\cdot}4 \quad \text{and} \quad 1{\cdot}0 < p < 3{\cdot}0;$$

(iii) The values selected in (i) and (ii) must satisfy (10) and (11).

2.3. *Comparisons with previous models*

Examination of this cascade model shows that both the Lyon (1982) and Dolmazon *et al.* (1977) models can be determined by reference to the constraining equations (10), (11), and (12). If the ratio L_T/L is assumed to be zero, then from (10) and (11) either $r = 1$ or $p = \infty$. Both these conditions yield a simplified cascade model.

Case 1

If $r = 1$ and p is finite, then (12) gives $Q_p = Q_z$. Since $r = 1$, $\omega_p = \omega_z$, thus the pole and zero functions in (4) cancel exactly. This leaves a cascade of simple low-pass filter functions which is similar to the cascade model proposed by Dolmazon *et al.* (1977).

Case 2

If $r = 1$ and $p \to \infty$, the low-pass filter in (4) can be omitted since its bandwidth is infinite. This leaves a cascade of pole/zero sections. However, the pole and zero functions will not cancel, since $Q_p \neq Q_z$. The result is a cascade of notch filters similar to the model proposed by Lyon (1982).

Case 3

The practical model proposed here assumes that the ratio L_T/L is finite, but small. Consequently, $r \neq 1$ and $p \neq \infty$.

2.4. *Digital filter model of the basilar membrane*

A digital filter model of the BM can be obtained by transforming the analogue filter equations (4) and (5) to equivalent digital filter equations. Since no attempt is made to model the phase response, we have chosen the impulse invariant transformation. This transformation should be applied to the model as a whole rather than to individual sections; however, the latter is found to be a good approximation.

On applying the impulse invariant transformation to (4), one obtains the pressure transfer function in the digital domain as given below:

$$\frac{v_o(z)}{v_i(z)} = K^* \frac{1-a_0}{1-a_0 z^{-1}} * \frac{1-b_1+b_2}{1-b_1 z^{-1}+b_2 z^{-2}} * \frac{1-a_1 z^{-1}+a_2 z^{-2}}{1-a_1+a_2}. \tag{13}$$

Similarly, the displacement transfer function in the digital domain is given by:

$$\frac{v_m(z)}{v_i(z)} = K^* \frac{1-a_0}{1-a_0 z^{-1}} * \frac{(1-b_1+b_2)z^{-1}}{1-b_1 z^{-1}+b_2 z^{-2}}, \tag{14}$$

where z is a complex variable and a_0, a_1, a_2, b_1, and b_2 are the digital filter coefficients.

One can see from (13) and (14) that the displacement transfer function is contained in the pressure transfer function and therefore a simple cascade arrangement is possible. Once the filter coefficients a_0, a_1, a_2, b_1, and b_2 have been calculated for each section of the BM, the filter structure shown in Fig. 5 can be implemented using the difference equations obtained by taking the inverse z-transform of (13).

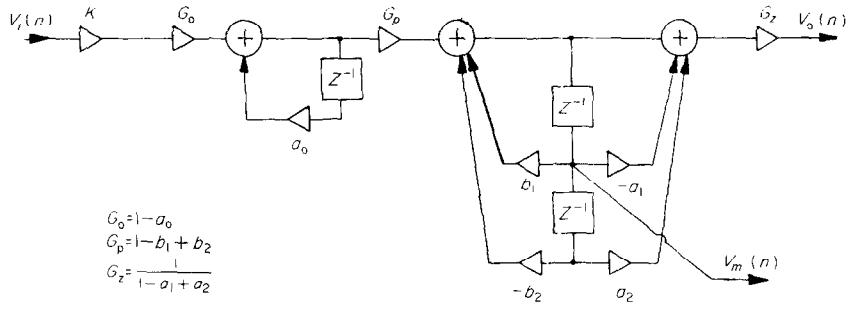

Figure 5. Digital filter realization of a basilar membrane section. $v_o(n)$ is the nth pressure output sample, $v_m(n)$ the nth displacement output sample, and $v_i(n)$ the nth input sample.

2.5. Selection of the frequency scale

The length of the BM is 3·5 cm. If it is simulated using 128 digital filters, connected in cascade with the sectional length, Δx, constant and given by

$$\Delta x = 3{\cdot}5/128 = 0{\cdot}0275 \text{ cm},$$

then the frequency ratio between adjacent sections is also constant throughout. According to Bekesy's frequency scale, if x is the distance of a point on the BM from the stapes, then the frequency, $f_p(x)$, that produces a peak at that point is given by:

$$f_p(x) = 16\,000 \times 10^{-0{\cdot}667x} \text{ Hz}, \tag{15}$$

where x is in centimetres. Hence,

$$\frac{[f_p(x)]_i}{[f_p(x)]_{i+1}} = \frac{16\,000 \times 10^{-0{\cdot}667x}}{16\,000 \times 10^{-0{\cdot}667(x+\Delta x)}}$$

$$= 10^{0{\cdot}667\Delta x} = 1{\cdot}043,$$

where i is the section number.

Table I shows the result obtained using Bekesy's frequency scale. It may be observed that if this scale is used then the spatial resolution will be poor. That is, the first 65 filters are spaced over 15 kHz (= 16 − 1·03 kHz) and the remaining 62 filters are spaced over 925 Hz (= 1003 − 75 Hz). In order to improve the spatial resolution and at the same time keep the number of filters fixed ($N = 128$), a new frequency scale had to be found.

TABLE I. Frequency resolution using Bekesy's frequency scale, illustrating the poor frequency resolution offered. Using this scale, the first 65 filters cover a 15 kHz frequency range, whereas the remaining 62 filters span the 925 Hz low-frequency range

Filter number	Distance (cm)	Frequency (f_p)
1	0	16 kHz
66	1·787	1·03 kHz
128	3·49	75 Hz

2.5.1 Mod-log scale

The modified scale is based on the relationship between the length and width of the BM. The BM varies in width and stiffness along its length. At the basal end it is narrow and stiff, whereas towards the apex, it is wider and more flexible. The width, $W_{BM}(x)$, of the BM along its length can be linearly approximated as:

$$W_{BM}(x) = 0{\cdot}019 + 0{\cdot}0093x \text{ cm}, \tag{16}$$

where x is the distance in centimetres from the base.

Thus, when $x = 0$, $W_{BM}(0) = 0{\cdot}019$ cm, and when $x = 3{\cdot}5$, $W_{BM}(3{\cdot}5) = 0{\cdot}05155$ cm.

It is assumed that each sectional length, Δx, varies in proportion to the width of the basilar membrane. That is:

$$\Delta x \propto W_{BM}(x).$$

What is required is the function y such that equal increments of Δy give increments Δx proportional to $W_{BM}(x)$. That is:

$$\Delta x = K_0 \Delta y W_{BM}(x). \tag{17}$$

Using (16) and (17) we obtain

$$\Delta y/\Delta x = 1/K_0 W_{BM}(x) = 1/K_0(0{\cdot}019 + 0{\cdot}0093x),$$

therefore,

$$y = \int [A/(1 + 0{\cdot}4895x)]\mathrm{d}x.$$

Hence,

$$y(x) = A\ ln(1 + 0{\cdot}4895x) + B,$$

where A and B are arbitrary constants. These constants can be evaluated using the following conditions:

when $y = 0$, $x = 0$, therefore $B = 0$;
when $y = 128$, $x = 3{\cdot}5$, therefore $A = 128{\cdot}238$.

The function $y(x)$ can now be completely defined as:

$$y(x) = 128{\cdot}238 \ln(1 + 0{\cdot}4895x), \tag{18}$$

where x is the distance from the base.

From (18), the distance of the ith and $(i+1)$th sections from the base can be calculated as follows:

$$x_i = \frac{\exp\left(\frac{y_i}{128{\cdot}238}\right) - 1}{0{\cdot}4895},$$

$$x_{i+1} = \frac{\exp\left(\frac{y_{i+1}}{128{\cdot}238}\right) - 1}{0{\cdot}4895},$$

therefore the width of the ith section is given by:

$$\Delta x_i = x_{i+1} - x_i = 0{\cdot}01599 \exp^{0{\cdot}007798_{yi}} \text{cm}, \tag{19}$$

where $y_i = 0{\cdot}5, 1{\cdot}5, 2{\cdot}5, \ldots, 127{\cdot}5$.

Equation (19) is referred to as the "mod-log" scale. Table II shows the spatial resolution result from the mod-log scale, and comparison with Table I illustrates the improvement in spatial resolution using the mod-log scale.

TABLE II. Frequency resolution using the "mod-log" scale. Comparison with Table I illustrates the improved frequency resolution, i.e. the first 80 filters cover a 15 kHz range and the remaining 47 filters span the 925 Hz low-frequency range

Filter number	Distance (cm)	Frequency (f_p)
1	0·0798	15·8 kHz
81	1·784	1·0 kHz
128	3·478	72 Hz

3. Results of the digital filter simulation

3.1. Values of the filter parameters

In order to simulate the basilar membrane vibration accurately, appropriate values of the filter parameters have to be chosen. One way of choosing the filter parameters is by applying (8)–(12), as explained previously in Section 2.2. The cochlea is represented as a cascade of 128 filters with the pole frequency (ω_p) of each filter calculated using (15). The resonant zero frequency (ω_z) is higher than the resonant pole (ω_p), but the actual frequency separation is unknown. One way of choosing the zero frequency is by the following relationship:

$$[\omega_z]_{i\text{th section}} = [\omega_p]_{(i-k)\text{th section}},$$

where $k = 1, 2, 3, \ldots$ In this case $k = 1$ is chosen.

In order to give appropriate amplitude enhancement at the pole frequency (ω_p) the value of r is calculated as follows:

$$[r]_{i\text{th section}} = [\{\omega_z/\omega_p\}]_{i\text{th section}}.$$

In addition, p needs to be estimated. A realistic value may be determined by choosing that p which will give model characteristics similar to those observed experimentally by Rhode (1971). In this case $p = 1{\cdot}6$ is chosen.

3.2. Results

Using the cochlea model it is possible to demonstrate many of the classical features described in the literature. One of the most fundamental observations is illustrated in Fig. 6. In this figure, the BM displacement is depicted in response to a 2 kHz tone (corresponding to a point 13 mm from the stapes) applied to the stapes. As expected, the

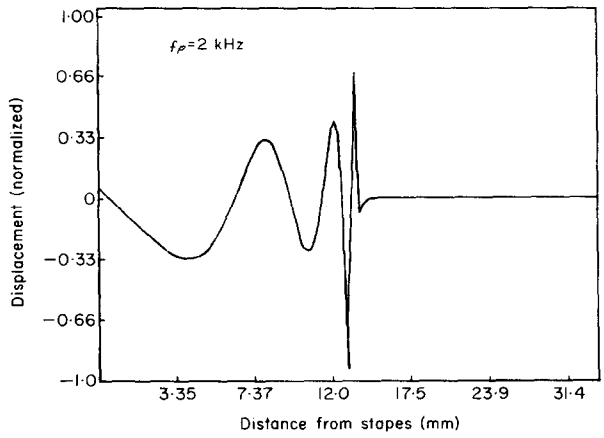

Figure 6. Displacement along the membrane due to a 2 kHz sine wave at the stapes, measured after a period of 20 ms. The model exhibits activity up to the point of resonance and none thereafter.

membrane exhibits moderate activity up to the characteristic frequency and maximum deflection occurs at the point of resonance. Beyond the point of resonance, no appreciable activity is observed. In terms of the pressure wave, therefore, it can be seen that it does not travel beyond the point of resonance. This result agrees with the findings of Zweig *et al.* (1976), who showed that the pressure wave propagates along the membrane being attenuated as it travels. At the place of resonance, the amplitude of the pressure wave must be zero and it cannot travel any further.

The frequency response of the model is obtained by taking the fast Fourier transform of the time derivated impulse response. To a first approximation, the cut-off rate of these curves is controlled by the Q-factor of the zero function, Q_z. The peak height and the sharpness of the peak are controlled by the Q-factor of the pole function, Q_p. As previously discussed in Section 3.1, the filter parameters have been estimated to obtain responses similar to measured responses. Figure 7 shows the frequency response of the model at a point along the membrane corresponding to a characteristic frequency of 7 kHz. By way of comparison, the response as found by Rhode (1971) is also given.

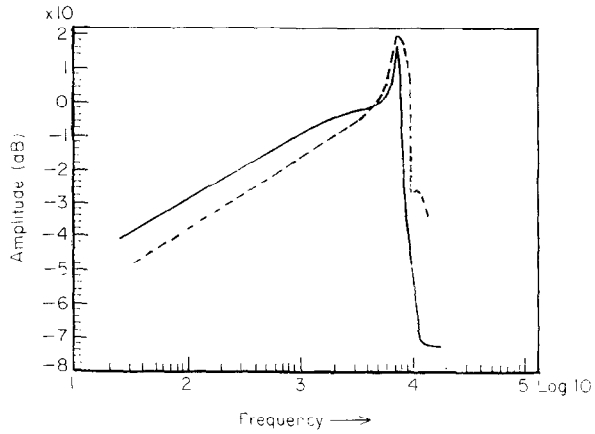

Figure 7. Frequency response of a point along the membrane whose characteristic frequency is 7 kHz (——). By way of comparison, the frequency response as measured by Rhode (1971) is shown (---).

4. Conclusion

A practical and computationally attractive model of the cochlea using digital simulation has been presented in this paper. A new design procedure is given to choose appropriate values of the filter coefficients in order to match the amplitude characteristics found empirically by Rhode (1971).

It is known that all existing mathematical and practical models of the BM motion are not able to match simultaneously the amplitude and phase characteristics found empirically by Rhode (1971). No attempt has been made in this model to satisfy the phase requirement. However, it does satisfy all the other requirements given in Section 1.

Recent measurements by Davis (1983), Kim (1985), and Neely (1985) indicate, as a result of the discovery of active elements, a very sharp tuning of the basilar membrane as compared to the earlier data observed by Rhode (1971). It is anticipated that this type of

sharp tuning of a particular membrane section could be obtained by the addition of feedback from basilar membrane displacement, $v_m(n)$, to the input, $v_i(n)$, outlined in Fig. 5 of this paper. This development, no doubt, will provide the basis for the implementation of the active cochlea.

References

Ambikairajah, E. & Linggard, R. (1984). Digital simulation of basilar membrane vibration. *International Conference AMSE-84*, Athens.

Black, N. D. (1983). Filterbank analysis of speech. PhD Thesis, Queen's University of Belfast.

Dallos, P. (1973). *The Auditory Periphery, Biophysics and Physiology*. Academic Press.

Davis, H. (1983). An active process in cochlear mechanics. *Hearing Research* **9**, 79–89.

Dolmazon, J. M., Bastet, L. & Shuplakov, V. S. (1977). A functional model of peripheral auditory system in speech processing. *Proceedings of the IEEE, ICASSP*, Hartford, 261–264.

Kim, D. O. (1985). A review of non-linear and active cochlear models. In *Peripheral Auditory Mechanisms*, **64** (J. B. Allen, J. L. Hall, Hubbard, S. T. Neely & A. Tubis, eds), pp. 239–249.

Lyon, R. F. (1982). A computational model of filtering detection and compression in the cochlea. *Proceedings of the IEEE, ICASSP*, Paris.

Neely, S. T. (1985). Mathematical modelling of cochlear mechanics. *Journal of the Acoustical Society of America* **78**(1), 345–352.

Rhode, W. S. (1971). Observation of the vibration of the basilar membrane of the squirrel monkey using the Mossbauer technique. *Journal of the Acoustical Society of America* **49**, 1218–1231.

Schroeder, M. R. (1973). An integratible model for the basilar membrane. *Journal of the Acoustical Society of America* **53**, 429–431.

Zweig, G., Lipes, R. & Pierce, J. R. (1976). The cochlear compromise. *Journal of the Acoustical Society of America* **59**, 975–982.